ELSEVIER

Physica B 322 (2002) 236–247

PHYSICA B

www.elsevier.com/locate/physb

The electronic properties of FeCo, Ni_3Mn and Ni_3Fe at the order–disorder transition

S.E. Kulkova[a,*], D.V. Valujsky[a], Jai Sam Kim[b], Geunsik Lee[b], Y.M. Koo[b]

[a] *Institute of Strength Physics and Materials Science of the Russian Academy of Sciences, pr. Akademichesky 2/1, 634021 Tomsk, Russia*
[b] *Department of Physics, Pohang University of Science and Technology, Pohang 790-784, South Korea*

Received 19 June 2001; accepted 20 February 2002

Abstract

Electronic structure calculations of the ordered ferromagnetic and paramagnetic transition metal alloys FeCo, Ni_3Fe and Ni_3Mn are performed using the full-potential linearized augmented plane wave method. The evolution of the electronic structure of alloys at disordering is studied in the framework of the Korringa–Kohn–Rostoker coherent potential approximation (KKR-CPA) combined with the local-density functional method. It is shown that the value of the magnetic moment is insensitive to order in all of the alloys investigated. The changes in the optical conductivity spectrum at the order–disorder transition are discussed.

PACS: 71.20.Be; 73.20.At; 78.20.Bh; 78.66.Bz

Keywords: Optical conductivity; Electronic structure; Alloys; Order–disorder transition

1. Introduction

The Fe- and Mn-based transition metal (TM) alloys possess a number of unusual physical properties, and have therefore been the subject of intense experimental and theoretical investigation [1–21]. However, in spite of the advances in knowledge about the electron properties of TM alloys, they are far from fully understood, even with regard to binary alloys. It is known that FeCo, Ni_3Fe and Ni_3Mn form ordered structures below some characteristic temperature, and can be ferromagnetic (FM). In particular, the ferromagnetic ordered B2 FeCo transforms at 1000 K into a ferromagnetic disordered BCC structure, and changes further at 1253 K into a paramagnetic (PM) disordered FCC structure. The lattice constant and magnetization of Fe–Co alloys depend non-monotonically on Co concentration, and change slightly upon ordering [1]. Experiments [1,2] indicate that the magnetic moment on the Co site changes only slightly over the entire concentration range, maintaining a value around $1.7\mu_B$, whereas the Fe magnetic moment increases dramatically from $2.2\mu_B$ for pure BCC Fe to $3.0\mu_B$ for ordered equiatomic FeCo. The high magnetic moment of FeCo suggests that the majority-spin states are almost completely full and the structure of the minority-spin bands is very important for FeCo.

*Corresponding author. Tel.: +7-382-2-258024; fax: +7-382-2-259576.

E-mail address: kulkova@ispms.tsc.ru (S.E. Kulkova).

0921-4526/02/$ - see front matter
PII: S0921-4526(02)01188-2

Ni_3Fe is ferromagnetic ordered below 776 K, but above 871 K it becomes paramagnetic. The Fe–Ni system displays many interesting properties; however, most attention has been focused on the Invar behavior of this alloy [3]. The crystal structure changes from BCC for the Fe-rich alloys to FCC for systems with higher Ni concentration. There is the complexity of the interaction between the magnetic and the compositional ordering [4,5]. Among others, Ni–Mn alloys have antiferromagnetic and ferromagnetic states, depending on the concentration of Mn [6]. Equiatomic NiMn has an antiferromagnetic ordered tetragonal structure below 980 K, but on increasing the Ni content up to 75% the Ni–Mn alloy becomes ferromagnetic ordered similar to the case of Ni_3Fe mentioned above. The magnetic properties of disordered Ni_3Mn are of interest. It has been argued that the disordered phase cannot be a simple paramagnetic phase [7]. In addition, it is known that the local magnetic properties of the magnetic TM alloys strongly depend on the local environment. The local moment disorder in Ni–Fe and Ni–Mn alloys has been previously considered in detail [8], and the electronic structure (ES) of Fe–Co, Ni–Fe and Ni–Mn has been investigated using a range of methods in a number of previous studies [3,7–18, and references therein]. In the case of Ni–Fe alloys, mainly the ES of the ordered Fe_3Ni alloy was studied [3]. Despite the difficulty of describing the electronic properties of random alloys, KKR-CPA calculations for Fe–Ni and Ni–Mn have been performed in Refs. [8,16,17]. These studies investigated the magnetic moment as a function of the concentration and volume. It should be noted that the calculation of the ES for the disordered FM alloys remains a very complicated task.

The electron properties in particular optical conductivity (OC) spectra have been experimentally studied for the ordered and disordered phases of both Ni_3Mn [19] and FeCo [20,21]. The optical data span all the states above and below the Fermi level (E_F). It would be useful to know if the theoretical methods used in the present paper give good results for the minority-spin states. In a previous paper [13], we studied the optical spectra in ordered and disordered FM FeCo. Unfortunately, the model Hamiltonian approximation within the non-self-consistent KKR method was used to calculate the band structure of the disordered phase, together with the constant matrix element approximation for OC. It is well known that the inclusion of the matrix element is very important for reliable comparison with experiment.

This paper reports the results of optical conductivity calculations for FeCo, Ni_3Mn and Ni_3Fe in both ordered and disordered phases. The magnetic properties are considered, and the changes in the electron properties at the order–disorder transition are discussed. The results obtained are compared with the available experimental data, and in general good agreement is found.

2. Computational details

The electronic structure calculations of ordered FeCo, Ni_3Mn and Ni_3Fe were performed using the full-potential linearized augmented plane wave (FLAPW) method [22] within the local spin density approximation (LSDA) and the generalized-gradient approximation (GGA) for the exchange-correlation potential [23]. The core states are fully relativistic, while the valence states including semi-core 3s, 3p states are treated as scalar relativistically. The wave function within the muffin-tin (MT) spheres was expanded in spherical-harmonics with angular momenta up to $l_{max}^{wf} = 10$. Non-spherical contributions to the charge density and the potential within the MT spheres were considered up to $l_{max} = 4$. In the interstitial region the plane waves with reciprocal lattice vectors up to $|G| = 14$ were included for the GGA. The band structure was calculated at 165 and 120 k-points in the irreducible part of the Brillouin zone (IP BZ) for FeCo and Ni_3Mn (Ni_3Fe), respectively. Self-consistency was considered to be achieved when the total energy variation from iteration to iteration did not exceed 10^{-5} Ry. A sphere radius of $R = 2.3$ a.u. was used for both components in all the systems investigated. In addition, the self-consistent KKR-CPA technique [24] was used to study the evolution of the electronic structure associated with the variation

in the composition and disordering. A brief description of this technique and more computational details for disordered magnetic TM alloys are given in Refs. [25,26]. The band structure was calculated at 506 and 161 k-points for disordered FeCo and Ni_3Mn (Ni_3Fe), respectively. The optical complex dielectric function and optical conductivity spectra in the energy range from 0 to 8 eV were calculated using the momentum matrix element, as described in detail elsewhere [22]. For optical properties of the ordered alloys the program within the framework of Wien 97 code has been applied. For the calculation of optical conductivity of the disordered alloys the Spicer equation was used as in Ref. [13]. The calculation of the optical properties requires a dense mesh of k-points. A range of k-mesh sizes (up to 1000 k-points in IP BZ) was used in the calculations. In general, use of a mesh finer than the 120–165 k-points modifies only slightly the intensities of the OC peaks and does not alter their positions.

3. Results and discussion

The optical conductivity spectra of Ni_3Mn and FeCo have been studied experimentally in both the ordered and disordered states [19–21]. However, to the best of our knowledge there are no experimental data for Ni_3Fe. In the measured energy range from 1 to 5 eV the interband transitions are predominant for both alloys. The optical conductivity spectrum of the ordered FM Ni_3Mn alloy shows a broad, pronounced peak at 1.66 eV. The disordering effect is basically the displacement of this peak to the lower energy of 1.4 eV. For ordered FM Ni_3Mn, a weak structure at 2.36 eV, which is absent in the OC of the disordered alloy, has also been pointed out [19]. A decrease in intensity at around 3.5 eV is observed in the experimental OC spectrum of disordered Ni_3Mn, whereas the OC of the ordered alloy has a plateau. In the infra-red (IR) region up to 1 eV there is a series of small peaks, which do not change significantly on disordering.

The displacement of the OC to lower energy is also observed for the B2 FeCo alloy at the order–disorder transition. Experimental OC spectra of this alloy show a two-band structure [20,21]. The first peak, at 1.4 eV, does not change at the FeCo order–disorder transition. The second peak shifts to the lower-energy region on disordering. The origin of the OC peculiarities has been discussed previously [13,21]. The conclusion reached was that electron transitions between states with opposite spins were the most reasonable explanation for the observed behavior [21]. Unfortunately, the data used in making this interpretation of the interband absorption were insufficient for analyzing even the optical properties of ordered FeCo. In addition, the conclusion that the shift of the high-energy peak is connected with the disappearance of the superlattice gaps at disordering [13] was based on non-self-consistent band structure results.

In order to understand the changes of the optical properties of FeCo, Ni_3Mn and Ni_3Fe, we first study the electronic structures of the ordered and disordered alloys and their changes at the magnetic transition.

3.1. FeCo

The total densities of states calculated for the disordered PM and FM FeCo alloy are shown in Fig. 1. This figure also includes the total spin density of states (DOS) for ordered FM FeCo, given by the dashed line. The Fermi level lies exactly at a sharp peak in the DOS for both the disordered and ordered PM FeCo. It is well known that a high DOS at the Fermi level may be an indication of unstable system. This result testifies against the paramagnetic ordered and disordered BCC structure for FeCo. We find that FeCo exhibits strong ferromagnetism in both the ordered and disordered phases. The majority-spin states are not very different for the ordered and disordered phases, in contrast to the minority-spin states. The DOS for minority spin is shifted to the high-energy region for ordered FeCo. Thus E_F is located in the valley between two main DOS peaks in ordered FM FeCo, but it lies in the local minimum of the DOS for minority spin in the disordered alloy. The high-energy peak in the DOS for the minority-spin states is smooth in the disordered phase. In general, our results for the

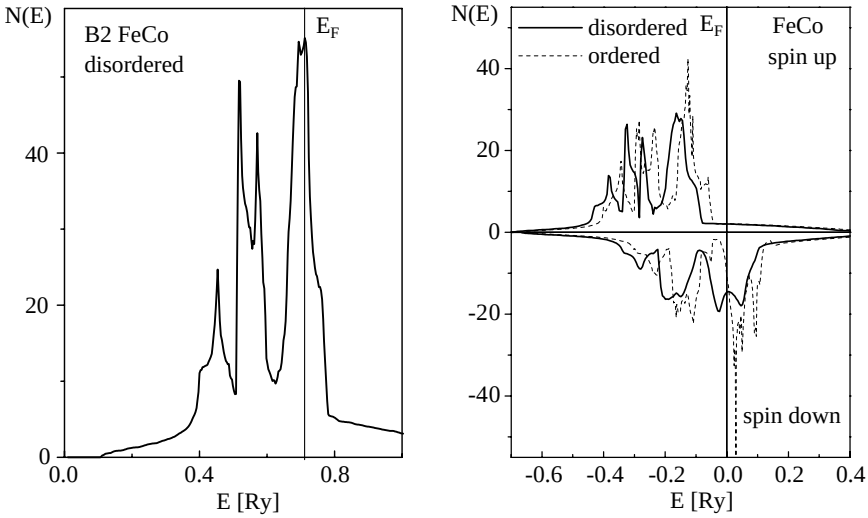

Fig. 1. Total DOS of disordered PM and FM B2 FeCo (DOS of the ordered FM alloy are given by dashed curves).

spin DOS for disordered FeCo differ from those of Desjonqueres and Lavagna [12]. However, the spin DOS for ordered FeCo is found to be in good agreement with earlier calculations [13–15]. The majority-spin states are fully occupied in the ordered and disordered phases. Exchange splitting of the states with opposite spin, together with the narrowing of the 3d-subbands, results in a large magnetic spin moment for the Fe and Co atoms (Table 1). The Co atom is more electronegative and has a smaller exchange splitting than Fe. For this reason, the Co minority-spin states lie at lower energy than the Fe states. In the minority-spin band structure of FeCo, the lower-energy bonding states have more Co character than Fe character, whereas the antibonding states (the states above the Fermi level) have more Fe weight.

We use the LSDA and GGA in the present calculations and find that the values obtained for the magnetic moment for ordered FeCo are in good agreement with the results of Liu and Singh [15], who also used the full-potential LAPW method. It should be noted that the magnetic properties of all investigated alloys were calculated at the experimental lattice constants. As seen from Table 1, the present calculations yield local spin moments that are slightly too large on the Co sites and slightly too small on the Fe sites for ordered FeCo, in comparison with the experimental results [2]. The GGA gives slightly larger values of the magnetic moment than the LSDA for both Co and Fe, as found previously [15]. At the same time, the radii of the atomic spheres are somewhat arbitrary but in the analysis of the experimental neutron data the Wigner–Seitz radii were used for the components of the alloy. Soderlind et al. [18] found that the orbital moment contributes only 3.1% of the total magnetic moment of FeCo. Our estimations within the GGA give the same result (Table 1). In order to reproduce accurately the orbital moments of transition metal alloys it is necessary that the orbital polarization effect will also be taken into account. As it was shown in Ref. [18] for FeCo the orbital moments of Fe and Co increase up to 0.092 and $0.106\mu_B$, respectively, i.e. they are approximately 50% larger than those in Table 1. We believe that this effect does not influence significantly the optical conductivity spectrum; therefore, it was not taken into account in the present calculations.

Experiments [1,2,27] show that the degree of order has only a relatively small influence on the magnetic moment. In the present study, the magnetic properties of FeCo change very little at

Table 1
Spin and orbital magnetic moments of ordered and disordered FeCo, Ni_3Mn and Ni_3Fe in μ_B

Alloys	State	Atom		μ (μ_B)-calculation	μ (μ_B)-experiment
FeCo	Ordered	Fe	Spin	2.74 (LSDA), 2.83 (GGA) (2.69[b,c], 2.78 and 2.84[d], 3.10[e,c]	2.92[a]
			Orbital	0.058 (0.065[c])	
		Co	Spin	1.77 (LDSA), 1.81 (GGA) (1.75[b], 1.71[c], 1.78 and 1.81[d], 1.60[e])	1.62[a]
			Orbital	0.071 (0.074[c])	
		Out		−0.07 (−0.04[b], −0.07[d])	
		μ-average		2.22 (2.25 and 2.27[d])	2.27[a,f]
	Disordered	Fe		2.65 (3.06[e])	3.0[g]
		Co		1.73 (1.64[e])	1.7[g]
		μ-average		2.18 (2.18[c])	
Ni_3Mn	Ordered	Mn	Spin	3.14 (LSDA), 3.31 (GGA) (3.22[h])	3.18[i]
			Orbital	0.01	
		Ni	Spin	0.52 (LSDA), 0.57 (GGA) (0.30[h])	0.30[i]
			Orbital	0.03	
		Out		−0.01, −0.06 (0.10[h])	
	Disordered	Mn		3.21	
		Ni		0.54	
Ni_3Fe	Ordered	Fe	Spin	2.87 (LSDA), 2.94 (GGA) (3.25[e])	2.97[i]
			Orbital	0.06	
		Ni	Spin	0.62 (LSDA), 0.66 (GGA) (0.62[e])	0.62[i]
			Orbital	0.04	
		Out		−0.09, −0.135	
	Disordered	Fe		2.81 (3.25[e])	
		Ni		0.57 (0.62[e])	
		($\mu_{Fe}-\mu_{Ni}$)		2.24	2.31[i]

In the calculations, local magnetic moments are given within the atomic inscribed spheres, while in the experiment, they are the moments within Wigner–Seitz sphere, (out) is the moment outside spheres.

[a] Ref. [2].
[b] Ref. [14].
[c] Ref. [18].
[d] Ref. [15].
[e] Ref. [12].
[f] Ref. [1].
[g] Ref. [27].
[h] Ref. [7].
[i] Ref. [29].

the order–disorder transition (see Table 1). The ordered FM state has a slightly larger total spin magnetization than the disordered FM state. The average magnetic moment in disordered FeCo ($2.18\mu_B$) is in good agreement with the result obtained previously using the virtual-crystal approximation (VCA) [18], which was adopted for an ES calculation of disordered FeCo. In this scheme, the atoms in the alloy are replaced by "average" atoms with nuclear charge $Z = 26.5$ and a valence electron number of $n_{val} = 8.5$. The coherent potential approximation is a much better scheme for calculating the electronic structure of the disordered alloys. The agreement between the present calculations and experiment [2] with regard to the E_g charge populations is also good. The E_g

fraction of the d-component of the charge densities in FeCo is 0.379 (0.37 [15]) and 0.352 (0.35 [15]) for Fe and Co, respectively, while the experimental result [2] is 0.384 for Fe and 0.343 for Co. The calculated E_g spin population around Co sites (0.63) is less than the experimental value of 0.69 [2], as found in Ref. [15]. Hence, the GGA does not lead to a significant change in the calculated spin density anisotropy in FeCo.

The trend obtained in the change of the total energy during the magnetic and order–disorder transitions is also in good agreement with previous studies [12,14]. For both ordered and disordered states the ferromagnetic phase corresponds to a lower energy than the paramagnetic phase. The values of the total energy for disordered PM and FM states are between those for the ordered phase. The total energy difference is 0.43 eV for the two disordered PM and FM phases. The values of the electronic specific heat coefficient from the DOS at the Fermi energy are 2.2 and 2.6 mJ mol^{-1} K^{-2} in the ordered and disordered FeCo. The experimental values [28] are 2.399 and 3.07 mJ mol^{-1} K^{-2}, respectively. The electronic specific heat coefficient decreases by 19% upon ordering. In general, our ES results are in reasonable agreement with experiment, as well as with the results from full-potential band structure calculations [15].

In Fig. 2 we present the calculated total optical conductivity for disordered FM FeCo (curve 1) and for ordered FM FeCo (curve 2), along with the experimental results of Kudryavtsev et al. [21] (curves 3 and 4). There is a fine structure on both theoretical curves at 1 eV and a minimum at 0.8 eV, which were not detected by experiment [21]. These features are, however, observed in the experimental curve for ordered FeCo in the work of Sasovskaja and Knyasev [20]. The high-energy peak at 2.3 eV (2.2 eV [13]) coincides very well with the experimental peak. For disordered FM FeCo, the change of the long-range order parameter causes the peak to be somewhat displaced to the low-energy region of 2.1 eV (1.9 eV in experiment [21]). A small shoulder at around 1.67 eV for the ordered FM alloy is more pronounced for the disordered FM state (1.5 eV). The structure of the OC for ordered FM FeCo is quite close to that

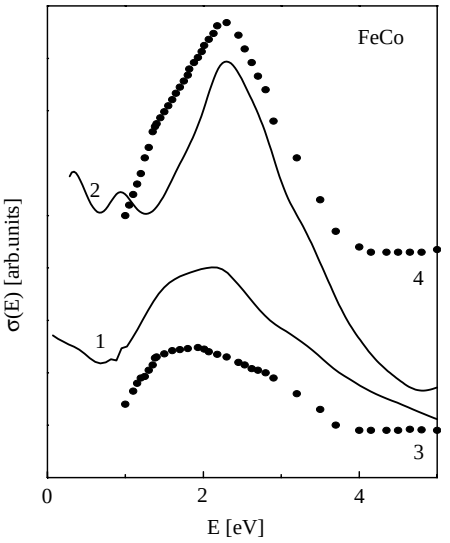

Fig. 2. The optical conductivity of FeCo: curves 1 and 2 are the theoretical $\sigma(E)$ for disordered and ordered FeCo, respectively, 3 and 4 are the experimental curves from Ref. [21].

found experimentally [20]. The width of the superlattice gaps obtained in the present calculation for ordered FeCo is slightly smaller than that obtained in our previous work [13] and experiment [21]. In general, the OC curve for the ordered alloy is displaced by a small amount to the high-energy region in comparison with the curve for the disordered alloy. The effect of the disappearance at disordering of the superlattice gaps at the boundary of the Brillouin zone, which leads also to the decrease in the bandwidth, could be responsible for the OC change at the order–disorder transition. The structure of the total optical conductivity spectrum is basically determined by the interband electron transitions between the minority-spin states. The contribution to the total OC of electron transitions between the majority-spin states is inessential because the DOS for the spin-up are almost completely occupied. The intraband transitions contribute mainly up to 1 eV. Unfortunately, the experimental spectra were measured only in the 1–5 eV energy region, hence we cannot compare our result in the IR region. The peak at 2.3 eV also coincides well with that for pure Fe. In general, we find a good agreement

between the experimental and theoretical results for both FeCo states. The most important result from the present calculations is the derivation of a reasonable ES for disordered FM FeCo, which allows us to reproduce well the optical conductivity spectrum for the disordered state.

3.2. Ni_3Fe and Ni_3Mn

The ordered Ni_3Mn alloy is ferromagnetic with an average magnetic moment of $1.02\mu_B$, in accordance with the experimental result of Schull and Wilkinson [29]. It is believed that the disordered alloy is essentially paramagnetic at room temperature, with possible weak ferromagnetism that depends on the state of disorder [29]. The magnetic structure of the disordered Ni–Mn alloys is not well characterized. It is supposed that each Mn atom has a magnetic moment of $4.0\mu_B$, but with random orientation. The magnetic properties of Ni–Mn alloys have been investigated in a number of other studies [6,30]. It has been suggested that when the Mn concentration is larger than 15% the magnetic states with the local moments parallel and antiparallel coexist, even in the ferromagnetic region [8]. Thus, the magnetic behavior of this system is very complicated.

Most studies of the electronic structure of Ni–Mn alloys have modeled an equiatomic alloy [7,31,32]. The calculated local spin DOS for the ordered FM Ni_3Mn alloy are given in Fig. 3. As in the case of FeCo, the majority-spin states are fully occupied. For the minority-spin states, the DOS has a dip between the two main peaks and the Fermi level is located slightly to the left side of this dip. The splitting of the local spin DOS for Ni and Mn shows that Mn basically determines the magnetic moment in the cell. The values obtained for the magnetic moment are in good agreement with experimental results [29] (Table 1). As shown in Fig. 3, the Mn minority-spin states are located above the Fermi level and are mainly antibonding in character. In the ferromagnetic Ni_3Fe alloy the splitting of the spin states is substantially less. The total and partial DOS for the ordered PM and FM Ni_3Fe are given in Fig. 4. The spin magnetic moment for the Fe atom ($2.87\mu_B$) is lower than that of the Mn atom. The magnetic moments for

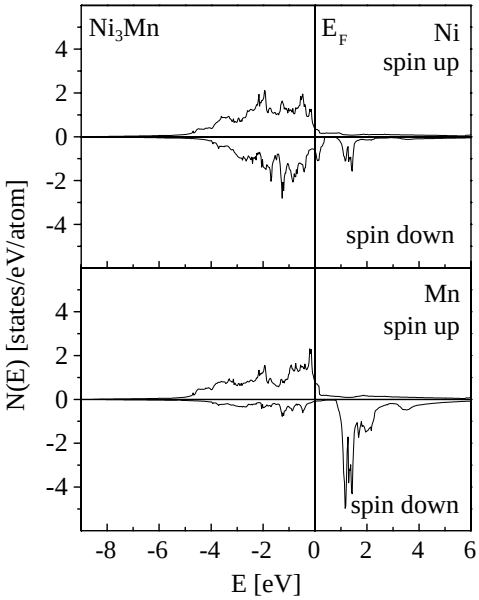

Fig. 3. Local spin DOS for ordered FM Ni_3Mn.

the Fe and Ni atoms are also in good agreement with experimental values [29]. In the present calculations we included the spin–orbit coupling, and the orbital moments were computed for both Ni_3Mn and Ni_3Fe alloys (Table 1). They are found to be in good agreement with the results obtained for the pure metals [33]. The results obtained indicate that indeed the effect of spin–orbit splitting is small in 3d systems, but must be considered to accurately describe the magnetic properties of TM alloys. Moreover, approximately double enhancement of the orbital moment at the surface was found recently in Ref. [33] for some magnetic 3d elements. However, the inclusion of the spin–orbit coupling did not affect some ground-state properties as it was shown in [33].

In the ordered PM structure of Ni_3Fe, and in that of Ni_3Mn, the Fermi level coincides exactly with a sharp peak in the DOS, as shown in Fig. 4. This peak is mainly due to the Fe states. However, E_F lies in the dip for the ordered FM structure, which has the lowest energy. It should be noted that in both Ni_3Mn and Ni_3Fe alloys the Fermi level lies near the peak that is located in the valley between the two main DOS peaks. Fig. 5 shows

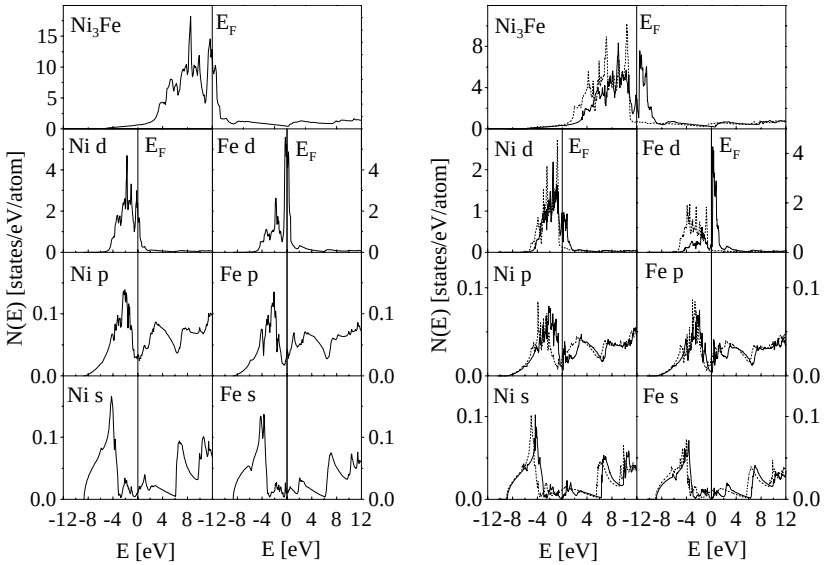

Fig. 4. Total and partial densities of states for ordered PM and FM Ni_3Fe.

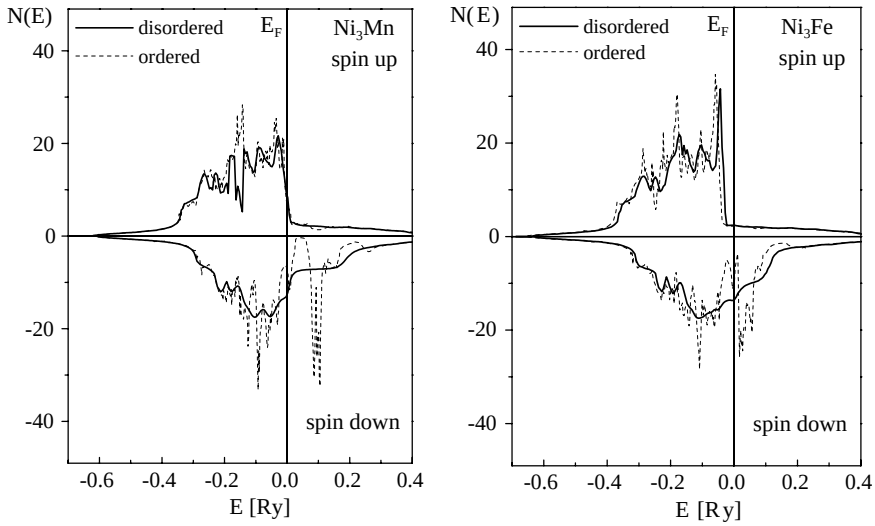

Fig. 5. Total DOS of disordered FM Ni_3Mn and Ni_3Fe (DOS of ordered FM alloys are given by dashed curves).

the total spin DOS for the ordered and disordered FM Ni_3Fe and Ni_3Mn alloys. A pronounced change in the DOS is observed at disordering. The high-energy peak of the minority-spin DOS is very smooth for both alloys. The calculated local magnetic moment for the Fe atom in the disordered FM Ni_3Fe alloy is less than that calculated by Desjonqueres and Lavagna [12]; however, the difference between the magnetic moments of the Fe and Ni atoms is in good agreement with experimental results [29,34]. On the basis of their experimental results for disordered Ni_3Fe, Schull and Wilkinson [29] conclude that the individual moments in disordered Ni_3Mn

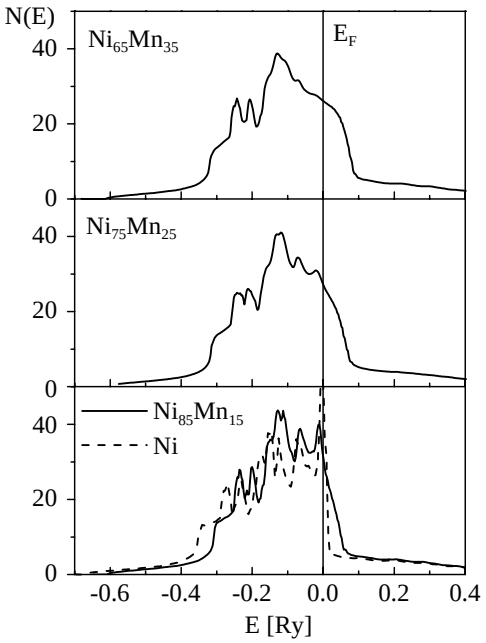

Fig. 6. Total DOS of the disordered PM Ni–Mn alloys depending on Mn concentration.

should not differ greatly from those in the ordered state. The results in Table 1 show that in both Ni_3Fe and Ni_3Mn, disordering indeed has little effect on the local magnetic moment. The local spin magnetic moment of Ni is overestimated in both ordered and disordered phases in Ni_3Mn, but is in good agreement with the experimental value for Ni_3Fe [29].

Because of the uncertainties in the electronic structure of disordered magnetic alloys, the electronic specific heat coefficient (γ) of both investigated alloys was also estimated. For ordered FM Ni_3Mn a value of $\gamma = 2.44\,\mathrm{mJ\,mol^{-1}\,K^{-2}}$ was obtained, which is lower than that of Yamashita et al. [7]. As mentioned above, in both ordered FM Ni_3Mn and Ni_3Fe alloys the Fermi level lies near a sharp peak and $N(E_F)$ changes substantially with increasing energy. The calculated value of $\gamma = 2.66\,\mathrm{mJ\,mol^{-1}\,K^{-2}}$ for disordered FM Ni_3Fe is in satisfactory agreement with the result of $3.0\,\mathrm{mJ\,mol^{-1}\,K^{-2}}$ [12], but is less than the experimental value of $3.88\,\mathrm{mJ\,mol^{-1}\,K^{-2}}$ [12]. We also estimated $N(E_F)$ and γ in disordered paramagnetic Ni–Mn alloys for Mn concentrations of 15%, 25% and 35% (Fig. 6). It was found that γ changed from 4.52 to $5.44\,\mathrm{mJ\,mol^{-1}\,K^{-2}}$ in going from 35% to 15% Mn. The Fermi level changes slightly with changing Mn concentration. As seen from Fig. 6, the total DOS shifts towards higher energy with increasing Mn concentration and $N(E_F)$ changes insignificantly, which is in good agreement with past results [7]. However, Proctor et al. report that γ rapidly increases with decreasing Mn concentration [35]. We conclude as in Ref. [7] that Ni_3Mn does not possess a simple disordered paramagnetic state. We also find that in the disordered state the ferromagnetic phase is more stable than the paramagnetic phase, although the energy difference is very small (0.054 eV for Ni_3Mn and 0.15 eV for Ni_3Fe). Furthermore, the ordered magnetic state is more stable than the disordered one, in accordance with the experimental observations for both Ni_3Fe and Ni_3Mn alloys.

Fig. 7 shows the calculated OC spectra for the ordered and disordered PM and FM Ni_3Fe and Ni_3Mn alloys. While E_F is located in the dip between two peaks for the minority-spin states, the structure of the OC is due to intensive interband transitions between the two different d-bands genetically connected with Ni and Mn (Fe). This results in the broad absorption band in the visible part of the spectrum with the peak at 1.75 eV on the theoretical OC for ordered FM Ni_3Mn. This is in good agreement with the experimental results [19]. The doublet peak, which is present in the theoretical curve, is shifted to slightly higher energy in comparison with the experimental peak at 1.66 eV. The different contributions to the total OC spectrum for ordered FM Ni_3Mn are shown in Fig. 8. The contribution from the transitions between the majority-spin states is small and does not influence the structure of the OC (Fig. 8). It is necessary to point out that the OC for ordered PM Ni_3Mn and Ni_3Fe has a maximum in the absorption near the Fermi level because E_F lies on a sharp peak in this case, as shown in Fig. 4. The doublet peak near E_F for ordered PM Ni_3Fe becomes a single peak on disordering and shifts slightly to lower energy. If we take into account the intraband transition (this contribution is not included in curves 1 and 3 in Fig. 7, lower panel),

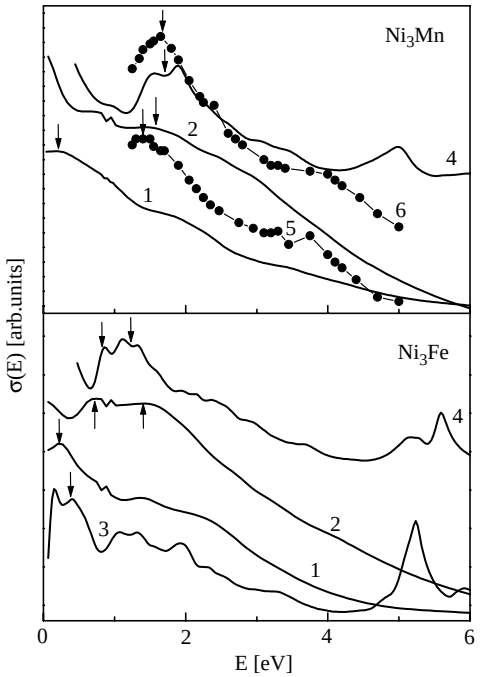

Fig. 7. The optical conductivity of Ni_3Mn and Ni_3Fe: curves 1 and 2 are theoretical $\sigma(E)$ for the disordered PM and FM alloys, respectively; 3 and 4 are $\sigma(E)$ for the ordered PM and FM alloys; 5,6 are experimental curves for disordered and ordered Ni_3Mn from Ref. [19].

the intensity of the OC sharply increases with decreasing energy. As a result, only weak features up to 1 eV could be detected in the IR region in the experiment. Hence, it is possible to discern the features in the region 1–3 eV for the paramagnetic state of Ni_3Fe, and the less pronounced structures in that region for disordered PM Ni_3Mn.

The structure of the OC for ordered FM Ni_3Fe is basically connected with the shape of the Fe band above E_F, which is a triplet and is significantly broader than the corresponding Mn band. In general, the absorption band for Ni_3Fe is shifted to the Fermi level because the Fe d-band is located closer to E_F than the Mn band in Ni_3Mn (Figs. 3 and 4). For ordered FM Ni_3Fe the first peak is located at around 0.85 eV and the doublet peak is at 1.25 eV. There is also a shoulder at 1.6 eV and a plateau at 1.9–2.8 eV, as in the theoretical and experimental curves for ordered

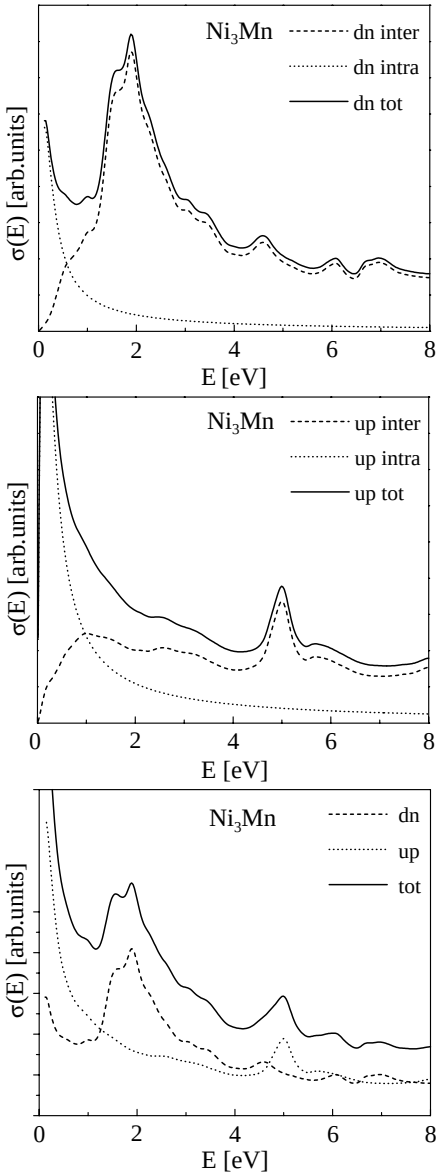

Fig. 8. The different contributions to the optical conductivity for ordered FM Ni_3Mn.

FM Ni_3Mn. The OC spectrum of the ordered FM Ni_3Fe alloy shows a more fine structure than that of Ni_3Mn. The minimum is located at 0.75 eV in Ni_3Fe and at 1.3 eV in Ni_3Mn. The intensity of the theoretical OC curves for ordered and disordered FM Ni_3Mn increases near the Fermi level, in good

agreement with the results [19]. Unfortunately, the contributions in the IR region found by Sasovskaja and Knjasev [19], given as the inset in Fig. 1 [19], could not be represented in Fig. 7. The absorption band of both disordered FM alloys has a weak feature at 1 eV. In addition, there is a broad band in the visible part of both spectra at approximately the same energy, as for the ordered FM alloys. The shape of this band for both disordered FM alloys is mainly due to the structure of the minority-spin DOS. Note that the theoretical OC obtained for the disordered FM alloys does not have any pronounced peculiarities in the region above 2 eV (only small shoulders), and cannot describe the fine structure at 3.5 eV in the experimental curve for disordered Ni_3Mn [19]. The OC for disordered FM Ni_3Fe has a minimum at 0.5 eV because the dip between the two d-bands below E_F is more pronounced in comparison with that for Ni_3Mn. The first peak in the visible part of the OC spectrum is shifted to slightly lower energy on disordering, whereas the second broad peak is displaced to higher energy. For Ni_3Mn the doublet peak becomes a singlet for the disordered FM phase and the spectrum is shifted to slightly lower energy.

In the work of Yamashita et al. [7], the Ni_3Mn DOS for minority-spin has a much more pronounced dip between d-subbands. In addition, these authors considered the so-called antiferromagnetic model for Ni_3Mn and found it to provide a better description of the magnetic structure of Ni–Mn alloys with high Ni concentrations [7]. Unfortunately, we could not use this model for Ni_3Mn within the KKR-CPA method. The investigation of the magnetic structure of transition metal alloys is a very complicated task. It is believed that the condition for ferromagnetism and antiferromagnetism in TM alloys is somewhat different from that in pure metals. The magnetic structure of Ni–Mn alloys depends very much on the Mn concentration, and moreover on the small concentration of the third element [36]. The changes in the optical properties of both the Ni_3Mn and Ni_3Fe alloys at disordering are connected with the smoother shape of the minority-spin DOS above the Fermi level for the disordered FM alloys. Sometimes the peculiarities of the OC are connected with the direct electronic transitions between the states in the high symmetry points or the direction of IP BZ. This approach cannot be correct, and it is necessary to calculate the partial optical densities of states to draw the final conclusion, as shown in our previous work [13]. The present result shows that the disordered structure of Ni_3Mn is not a simple paramagnetic one. At the same time, the calculated OC spectrum for the disordered ferromagnetic Ni_3Mn alloy is slightly different from the experiment. The experimental spectrum shows a much more pronounced separation in the DOS structure near the Fermi level.

4. Summary

In the present work, we have calculated the electronic structure and optical properties for some transition metal alloys in their ordered and disordered phases. The change in the electronic structure at the magnetic transition was also studied. We have found that the spin magnetic moments for all investigated transition metal alloys are insensitive to order, in contrast to their densities of states, which vary significantly with order. The calculated values of the spin magnetic moment are in good agreement with the available experimental results. The magnitudes of the orbital moments have also been estimated for all of the alloys investigated, and a small effect of spin–orbit splitting was found. It is shown that for ordered and disordered ferromagnetic alloys the interband transitions between the minority-spin states provide the main contribution to the total optical conductivity. The calculated optical spectra for FeCo are found to be in good agreement with the experiment for both the ordered and disordered phases. The change of OC in the visible part of the spectrum for disordered FM Ni_3Fe and Ni_3Mn alloys is due to the minority-spin density of states above the Fermi level. A less prounounced minimum between the d-bands for the minority-spin DOS of disordered Ni_3Mn is found in the present ferromagnetic calculation. The magnetic structure of the Ni–Mn alloys with a high concentration of Ni could be more complicated

than the ferromagnetic structure, which was considered here. The result obtained for a simple paramagnetic model for the disordered Ni_3Mn alloy disagrees with the experimental optical conductivity spectrum.

Acknowledgements

This work was partly supported by a collaborative program between the Institute of Strength Physics and Materials Science RAS, Tomsk, Russia and the Basic Science Research Institute, Pohang University of Science and Technology, Republic of Korea. The research was also jointly funded by the KOSEF-2001 research fund. S.K. thanks A.F. Tatarchenko and N.I. Kulikov for allowing the use of the KKR-CPA code for the calculations.

References

[1] D.J. Bardos, J. Appl. Phys. 40 (1969) 1371.
[2] E. Di Fabrizio, B. Mazzone, C. Petrillo, F. Sacchetti, Phys. Rev. B 40 (1989) 9502.
[3] I.A. Abrikosov, O. Eriksson, P. Soderlind, Phys. Rev. B 51 (1995) 1058.
[4] M.Z. Dang, D.G. Rancourt, Phys. Rev. B. 53 (1996) 2291.
[5] J.B. Staunton, D.D. Johnson, B.L. Gyorffy, J. Appl. Phys. 61 (1987) 3693.
[6] Y. Kitaoka, K. Asayama, J. Phys. Soc. Japan 40 (1976) 1521.
[7] J. Yamashita, S. Asano, S. Wakoh, Progr. Theor. Phys. 47 (1972) 774.
[8] H. Akai, P.H. Dederichs, Phys. Rev. B 47 (1993) 8739.
[9] J. Yamashita, S. Wakoh, S. Asano, J. Phys. Soc. Japan 21 (1966) 53.
[10] H. Hasegawa, J. Kanamori, J. Phys. Soc. Japan 33 (1971) 1599.
[11] T. Jo, J. Phys. Soc. Japan 40 (1976) 715.
[12] M.C. Desjonqueres, M. Lavagna, J. Phys. F 9 (1979) 1733.
[13] S.E. Kulkova, V.E. Egorushkin, I.N. Anokhina, V.P. Fadin, Phys. Stat. Sol. B 103 (1981) 653.
[14] K. Schwarz, P. Mohn, P. Blaha, J. Kubler, J. Phys. F 14 (1984) 2659.
[15] A.Y. Liu, D.J. Singh, Phys. Rev. B 46 (1992).
[16] D.D. Johnson, F.J. Pinski, G.M. Stocks, J. Appl. Phys. 57 (1987) 3018.
[17] D.D. Johnson, F.J. Pinski, J.B. Staunton, J. Appl. Phys. 61 (1987) 3715.
[18] P. Soderlind, O. Eriksson, B. Johansson, R.C. Albers, A.M. Boring, Phys. Rev. B 45 (1992) 12911.
[19] I.I. Sasovskaja, Yu.V. Knjasev, Vliyanie uporyadocheniya na opticheskiee svoistva splava Ni3Mn//Electronnaya structura perehodnih metallov ih splavov i intermetallicheskih soedinenii. Kiev, Naukova Dumka, 1979, p. 89.
[20] I.I. Sasovskaja, Yu.V. Knyasev, Zh. Prikl. Spektrosk. 28 (1978) 564.
[21] Yu.V. Kudryavtsev, I.V. Lezhnenko, A.G. Lesnik, Fiz. Met. Metalloved. 47 (1979) 747.
[22] P. Blaha, K. Schwarz, J. Luitz, WIEN97, Vienna University of Technology, 1997, 161pp. (Improved and updated Unix version of the origin copyrighted WIEN-code, which was published by P. Blaha, K. Schwarz, P. Sorantin, S.B. Trickey, in Comput. Phys. Commun. 59 (1990) 399).
[23] J.D. Perdew, K. Burke, M. Ernzerhof, Phys. Rev. Lett. 77 (1996) 3865.
[24] A.F. Tatarchenko, N.I. Kulikov, Phys. Rev. B 50 (1994) 8266.
[25] N.I. Kulikov, C. Demangeat, Phys. Rev. B 55 (1997) 3533.
[26] N.I. Kulikov, A.V. Posnikov, G. Borstel, J. Braun, Phys. Rev. B 59 (1999) 6824.
[27] S. Spooner, J.W. Lynn, J.W. Cable, AIP Conf. Proc. 5 (1971) 1415.
[28] R. Kuentzler, Phys. Stat. Sol. B 58 (1973) 519.
[29] C.G. Schull, M.K. Wilkinson, Phys. Rev. 97 (1955) 305.
[30] H. Tange, T. Tokunaga, M. Goto, J. Phys. Soc. Japan 45 (1978) 105.
[31] S.E. Kulkova, V.V. Kalchikhin, Izv. Vyssh. Uchebn. Zaved., Fiz. 8 (1991) 18.
[32] A. Sakuma, J. of Magnetism, Magn. Mater. 187 (1998) 105.
[33] O. Eriksson, A.M. Boring, R.C. Albers, G.W. Fernando, B.R. Cooper, Phys. Rev. B 45 (1992) 2868.
[34] M. Nishi, Y. Nakai, N. Kunitomi, J. Phys. Soc. Japan 37 (1974) 570.
[35] W. Proctor, R.G. Scurlock, E.M. Wray, Proc. Phys. Soc. 90 (1967) 697.
[36] V.E. Egorushkin, S.E. Kulkova, S.N. Kulkov, Zh. Eksp. Teor. Fiz. (Sov. Phys.-JETP). 84 (1983) 599.